Hindawi
Discrete Dynamics in Nature and Society
Volume 2022, Article ID 4798415, 17 pages
https://doi.org/10.1155/2022/4798415

Research Article

Further Improvement on Stability Results for Delayed Load Frequency Control System via Novel LKFs and Proportional-Integral Control Strategy

Xingyue Liu,[1] Kaibo Shi ,[1,2,3] Lin Tang ,[1] and Yiqian Tang[1]

[1]*School of Electronic Information and Electrical Engineering, Chengdu University, Chengdu 610106, China*
[2]*Engineering Research Center of Power Quality of Ministry of Education, Anhui University, Hefei 230601, China*
[3]*Institute of Electronic and Information Engineering of University of Electronic Science and Technology of China, Guangdong 523808, China*

Correspondence should be addressed to Kaibo Shi; skbs111@163.com

Received 6 March 2022; Accepted 24 March 2022; Published 9 May 2022

Academic Editor: Zi-Peng Wang

In this work, novel stability results for load frequency control (LFC) system considering time-varying delays, nonlinearly perturbed load, and time-varying disturbance of system parameters are proposed by using proportional-integral control strategy. Considering the nonlinearly exogenous load disturbance and system parameters disturbance, an improved stability criterion in the form of linear matrix inequalities (LMIs) is derived by novel simple Lyapunov–Krasovskii functionals (LKFs). The delay-dependent matrix in quadratic term, cross terms of variables, and quadratic terms multiplied by 1st, 2nd, and 3rd degrees of scalar functions are included in the new simple LKF. Taking the single-area and two-area LFC system installed with proportional-integral (PI) controller as example, our results surpass the previous maximum allowable size of time delay. Meanwhile, the relationship between time delay varying rate, load disturbance degree, gains of PI controller, and delay margin of the LFC system is researched separately. The results can provide guidance to tune the PI controller for achieving maximum delay margin, in which the LFC system can withstand without losing stability. At last, the simulation results verify the effectiveness and superiority of the proposed stability criterion.

1. Introduction

The usage of load frequency control (LFC) is widely in the power system, which restores the balance of the power system between load demand and generation supply [1–3]. The sudden change of load can bring threaten to the safe and economic operation of the power system. Thus, the analysis and research about LFC scheme of the power system are considered to be essential and important segment to guarantee the safe operation of the power system. The LFC scheme is also effectively applied in smart grid [4, 5].

A wide and dedicated open communication network is needed to transmit control signals, measurements between remote RTUs, and the control center in the conventional LFC system [3, 6]. The usage of the communication network leads to a series of inevitable problems, like time delays [7–11], packet losses, and so on. Hence, many researchers focus on the time delay phenomenon of the power control system and the impact of network delay on the communication-based power system [12–16]. From the perspective of stability analysis, it is of significant to seek the maximum allowable network delay that the power system with LFC scheme can withstand without losing sable.

Generally speaking, there are mainly two approaches to seek the upper bound of the time delay system, which have different restriction and conservatism. One is the direct approach, which is frequency domain method, such as tracing eigenvalue [17, 18], or cluster treatment of characteristic roots [19–21]. The advantage of these direct methods is that the accurate delay margin can be derived by

calculating eigenvalues of the whole system. However, the disadvantage of direct methods is that they can only be applied to constant time delays situation. The other is time domain method, which is based on Lyapunov stability theory and linear matrix inequalities (LMIs) techniques [22–26]. Though the time domain methods are more conservatism than the frequency domain methods, the time domain methods can be applied in both constant and time-varying delays situation. So, the time domain methods based on Lyapunov stability theory are abroad exploited.

The main effort to diminish the conservatism of time domain methods has focused on two aspects, methods of constructing L-K functional and analyzing techniques for bounding the derivatives of L-K functional with regard to time. The former includes delay-division functional, functional with matrices dependent on the time delays [27], functional with two-integral or triple-integral terms [28], and so on. The latter techniques include improved majorization technique, free weighting matrix method [29], integral inequality including Jesen inequality [23], Wirtinger inequality [30], auxiliary function-based integral inequality [31], and reciprocal convex technique [32]. More and more researchers focus on the delay-dependent criteria for stability of the power system because the delay-dependent criteria have less conservatism than delay-independent criteria [22, 33].

Until now, there are a few excellent research studies about stability analysis of the delayed LFC systems. Ramakrishnan and Ray [34] focused on the delay-dependent robust stability problem for the LFC system with multiple time-invariant delays in H_∞ framework. The model of the LFC system with both sampling and transmission delay was proposed in [35]. The stability analysis problem was considered in [3], which focused on the LFC system with electric vehicles and time delays. The novel linear operator inequality approach was proposed, and a delay-dependent stability criterion with less conservative was obtained. Unfortunately, the load disturbance and random disturbance of system parameters were not considered either in the stability analysis or simulation in the above literatures. It is worth noting that the bounded nonlinear load perturbation model was built without considering random disturbance of system parameters in literatures [22, 36, 37]. The augmented L-K functional including single and double integral terms was developed to analyze stability of the LFC system in these literatures. The novel LKF with delay-dependent matrix in quadratic term, cross terms of variables, and quadratic terms multiple by a higher degrees of scalar function proposed by this paper contains more information about state variables than the routine L-K functional adopted in [22, 36, 37], and the results in this paper are less conservative than those of [22, 36, 37].

This work proposes a novel stability criterion for the time-varying delay LFC power system considering nonlinearly perturbed and random disturbance of system parameters. Considering unknown exogenous load disturbance and random disturbance of system parameters as constrained time-varying nonlinear function related to current and delayed state vectors, the delayed LFC system with PI controller can be described as a time-varying delay system. Then, the novel stability criterion of the LFC power system is expressed in the form of LMIs by a simple LKF and integral inequalities. The main opinion of constructing the new LKF is the application of delay-dependent matrix, cross terms of variables, and quadratic terms multiplied by 1st, 2nd, and 3rd degrees of scalar function. Moreover, the case studies are carried out taking the single-area and two-area LFC system installed with PI controller as example with simulation examples to verify the effectiveness and superiority of the proposed stability criteria.

2. System Description and Problem Formulation

The notations of jth area for the LFC system are given in Table 1. The subscript j should be omitted for the single-area LFC system. For example, K_{Pi} can be changed to K_P in the single-area LFC system. It is worth noting that $\Delta P_{tie} = 0$ in the single-area LFC system.

Consider the uncertainties in the power parameters of the actual LFC system. The state-space model with disturbance parameters and load disturbance of the multiarea LFC system (N area) is presented as follows:

$$\begin{cases} \dot{x}(t) = (A + \Delta A(t))x(t) + \sum_{j=1}^{N}\left(B_j + \Delta B_j(t)\right)x\left(t - h_j(t)\right) + C\Delta L_{\mathrm{d}}(t), \\ x(t) = \phi(t),\ t \in \left[-\max\left(h_j(t)\right), 0\right], \end{cases} \tag{1}$$

where $x(t)$ represents state vector. A and B represent the system matrices related to the current state and delayed state vectors. $\Delta A(t) = \mathrm{NF}(t)D_1$ and $\Delta B(t) = \mathrm{NF}(t)D_2$ represent perturbation parameters. $F(t)$ is a time-varying matrix, which satisfies $F^T(t)F(t) \le I$. N, D_1, and D_2 are the constant matrix. $h_j(t)$ represents the network time-varying delay in j th area. C represents the known matrix related to the disturbance vector. The initial state can be described by a continuous function defined in $t \in [-\max(h_j(t)), 0]$.

2.1. LFC Modeling. In order to simplify the calculation, it supposes that $h_j(t) = h(t)$, which means the multiple delays are supposed to be equal and shown as a unified time-

Table 1: Notations.

Δf_j	Deviation of frequency	K_{Pj}	Proportional gain	K_{Ij}	Integral gain
ACE_j	Area control error	ΔL_{dj}	Disturbance of load	D_j	Damping constant
M_j	Generator inertia moment	T_{tj}	Turbine time constant	T_{gj}	Time-constant
γ_j	Frequency bias factor	ΔP_{tie}	Tie-line power transfer	ΔP_{mj}	Generator output
ΔP_{vj}	Generator valve position	$\widehat{v}_j$	Speed drop	R_{ij}	Synchronize coefficient

varying delay $h(t)$. So, the state-space model of multiple-area can be presented as follows:

$$\begin{cases} \dot{x}(t) = (A + \Delta A(t))x(t) + (B + \Delta B(t))x(t - h(t)) + C\Delta L_d(t) \, (0 \le h(t) \le h, -\mu \le \dot{h}(t) \le \mu), \\ x(t) = \phi(t), \quad t \in [-h, 0], \end{cases} \tag{2}$$

where $B = \sum_{i=1}^{n} B_i$ and $\Delta B(t) = \sum_{i=1}^{n} \Delta B_i(t)$. h and μ represent the upper bound of time-varying delay and the delay derivative separately. The constraints of $h > 0$ and $0 < \mu < 1$ can make time-varying delay systems well-posed because the fast time-varying delay will cause a series of problems, like causality, minimality, inconsistency, and so on.

Furthermore, considering $\Delta A(t) = \mathrm{NF}(t)D_1$ and $\Delta B(t) = \mathrm{NF}(t)D_2$, the state-space model of multiple-area can be rewritten as follows:

$$\begin{cases} \dot{x}(t) = Ax(t) + Bx(t - h(t)) + C\Delta L_d(t) + \mathrm{NF}(t)\left(D_1 x(t) + D_2 x(t - h(t))\right) (0 \le h(t) \le h, -\mu \le \dot{h}(t) \le \mu), \\ x(t) = \phi(t), \quad t \in [-h, 0]. \end{cases} \tag{3}$$

For a typical two-area LFC system, the dynamic model is shown in Figure 1. $e^{-sh(t)}$ is network time-varying delay notation. The state vectors, load disturbance vectors, and system matrices are presented as follows:

$$x(t) = \left[\Delta f_1(t) \;\; \Delta P_{m1}(t) \;\; \Delta P_{v1}(t) \;\; \int \mathrm{ACE}_1(t)\mathrm{d}t \;\; \Delta P_{12}(t) \;\; \Delta f_2(t) \;\; \Delta P_{m2}(t) \;\; \Delta P_{v2}(t) \;\; \int \mathrm{ACE}_2(t)\mathrm{d}t \right]^T,$$

$$A = \begin{bmatrix} -\frac{D_1}{M_1} & \frac{1}{M_1} & 0 & 0 & -\frac{1}{M_1} & 0 & 0 & 0 & 0 \\ 0 & -\frac{1}{T_{t1}} & \frac{1}{T_{t1}} & 0 & 0 & 0 & 0 & 0 & 0 \\ -\frac{1}{\widehat{v}_1 T_{t1}} & 0 & -\frac{1}{T_{t1}} & 0 & 0 & 0 & 0 & 0 & 0 \\ \gamma_1 & 0 & 0 & 0 & 1 & 0 & 0 & 0 & 0 \\ 2\pi R_{12} & 0 & 0 & 0 & 0 & -2\pi R_{12} & 0 & 0 & 0 \\ 0 & 0 & 0 & 0 & \frac{1}{M_2} & \frac{-D_2}{M_2} & \frac{1}{M_2} & 0 & 0 \\ 0 & 0 & 0 & 0 & 0 & 0 & -\frac{1}{T_{t2}} & \frac{1}{T_{t2}} & 0 \\ 0 & 0 & 0 & 0 & 0 & -\frac{1}{\widehat{v}_2 T_{t2}} & 0 & -\frac{1}{T_{t2}} & 0 \\ 0 & 0 & 0 & 0 & -1 & \gamma_2 & 0 & 0 & 0 \end{bmatrix},$$

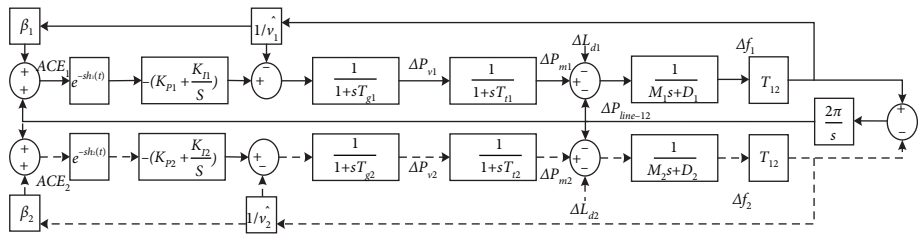

Figure 1: Dynamic model of two-areas LFC scheme and single-area without dotted lines.

$$B=\begin{bmatrix} 0 & 0\ 0 & 0 & 0 & 0 & 0\ 0 & 0\ 0 & 0\\ 0 & 0\ 0 & 0 & 0 & 0 & 0\ 0 & 0\ 0 & 0\\ -\frac{\gamma_1 K_{P1}}{T_{g1}} & 0\ 0 & -\frac{K_{I1}}{T_{g1}} & -\frac{K_{P1}}{T_{g1}} & 0 & 0\ 0 & 0\\ 0 & 0\ 0 & 0 & 0 & 0 & 0\ 0 & 0\ 0 & 0\\ 0 & 0\ 0 & 0 & 0 & 0 & 0\ 0 & 0\ 0 & 0\\ 0 & 0\ 0 & 0 & 0 & 0 & 0\ 0 & 0\ 0 & 0\\ 0 & 0\ 0 & 0 & 0 & 0 & 0\ 0 & 0\ 0 & 0\\ 0 & 0\ 0 & 0 & \frac{K_{P2}}{T_{g2}} & -\frac{\gamma_2 K_{P2}}{T_{g2}} & 0\ 0 & -\frac{K_{I2}}{T_{g2}}\\ 0 & 0\ 0 & 0 & 0 & 0 & 0\ 0 & 0\ 0 & 0 \end{bmatrix},$$

$$C=\begin{bmatrix} -\frac{1}{M_1} & 0\ 0\ 0 & 0 & 0\ 0\ 0\ 0\\ 0 & 0\ 0\ 0 & -\frac{1}{M_2} & 0\ 0\ 0\ 0 \end{bmatrix}^T \quad \Delta L_{\mathrm{d}}(t)=\left[\Delta L_{\mathrm{d1}}(t)\ \ \Delta L_{\mathrm{d2}}(t)\right]^T F(t) \quad =\left[F_1(t)\ \ F_2(t)\right]^T. \tag{4}$$

For the j th area, $j = 1, 2$, the notations are presented in Table 1.

The dynamic model of the single-area LFC system is shown in Figure 1 without dotted lines. The state vector, disturbance vector, and system matrices of the single-area LFC system are reduced as follows:

$$x(t)=\left[\Delta f(t)\ \ \Delta P_m(t)\ \ \Delta P_v(t)\ \ \int \mathrm{ACE}(t)\mathrm{d}s\right]^T,$$

$$A=\begin{bmatrix} -\frac{D}{M} & \frac{1}{M} & 0 & 0\\ 0 & -\frac{1}{T_t} & \frac{1}{T_t} & 0\\ -\frac{1}{\hat{v}T_g} & 0 & -\frac{1}{T_g} & 0\\ \gamma & 0 & 0 & 0 \end{bmatrix},$$

$$B=\begin{bmatrix} 0 & 0\ 0 & 0\\ 0 & 0\ 0 & 0\\ -\frac{\gamma K_P}{T_g} & 0\ 0 & -\frac{K_I}{T_g}\\ 0 & 0\ 0 & 0 \end{bmatrix}, \tag{5}$$

$$\Delta L_d(t)=\left[\Delta L_d(t)\right]^T F(t)=\left[F(t)\right]^T,$$

$$C=\begin{bmatrix} -\frac{1}{M} & 0 & 0 & 0 \end{bmatrix}^T.$$

Remark 1. When there are $N\,(N > 1)$ subareas connected by tie-lines forming a multiarea power system, the dotted line will be copied by N times. The decentralized control strategy is applied in the multiarea power system, which means every control area is independent and has its own LFC center to maintain the balance of generation and load. As a result, the interactions between i th area and other areas,

$\sum_{j=1,j\neq i}^{N} T_{ij}\Delta f_j$, are treated as disturbances for i th area. Then, define $x_i(t) = \mathrm{col}\left\{\Delta f^T \Delta P_{mi}^T \Delta P_{vi} \int \mathrm{ACE}_i^T \Delta P_{\mathrm{line}-i}^T\right\}$, where (4) is the expanded form of $x_i(t)$ in two-area power system. And the system matrices of multiareas are listed as follows:

$$A = \begin{bmatrix} A_{11} & A_{12} & \cdots & A_{1N} \\ A_{21} & A_{22} & \cdots & A_{2N} \\ \vdots & \vdots & \ddots & \vdots \\ A_{N1} & A_{N2} & \cdots & A_{NN} \end{bmatrix},$$

$$A_{ii} = \begin{bmatrix} -\frac{D_i}{M_i} & \frac{1}{M_i} & 0 & 0 & -\frac{1}{M_i} \\ 0 & -\frac{1}{T_{chi}} & \frac{1}{T_{chi}} & 0 & 0 \\ -\frac{1}{R_i T_{gi}} & 0 & -\frac{1}{T_{gi}} & 0 & 0 \\ \beta_i & 0 & 0 & 0 & 1 \\ 2\pi\Sigma_{k=1,k\neq i}^{N} T_{ik} & 0 & 0 & 0 & 0 \end{bmatrix},$$

$$A_{ik} = \begin{bmatrix} 0 & 0 & 0 & 0 & 0 \\ 0 & 0 & 0 & 0 & 0 \\ 0 & 0 & 0 & 0 & 0 \\ 0 & 0 & 0 & 0 & 0 \\ 2\pi T_{ik} & 0 & 0 & 0 & 0 \end{bmatrix},$$

$$B = \mathrm{diag}\{B_1, B_2, \ldots, B_N\},$$

$$B_i = \begin{bmatrix} 0 & 0 & \frac{1}{T_{gi}} & 0 & 0 \end{bmatrix}^T,$$

$$C = \mathrm{diag}\{C_1, C_2, \ldots, C_N\},$$

$$C_i = \begin{bmatrix} \beta_i & 0 & 0 & 0 & 1 \\ 0 & 0 & 0 & 1 & 0 \end{bmatrix}, \tag{6}$$

$$F = \mathrm{diag}\{F_1, F_2, \ldots, F_N\},$$

$$F_i = \begin{bmatrix} -\frac{1}{M_i} & 0 & 0 & 0 & 0 \end{bmatrix}^T,$$

$$\Delta L_{\mathrm{d}}(t) = \mathrm{dig}\{\Delta L_{\mathrm{d1}}(t) \ldots \Delta L_{\mathrm{di}}(t)\}.$$

2.2. Disturbance Parameters and Load Disturbance Model of LFC System. This paper models the unknown disturbance of power system parameters as $\mathrm{NF}(t)(D_1 x(t) + D_2 x(t - h(t))) = Np(t, x(t), x(t - h(t)))$, which is nonlinear function related to current and delayed state vector. Owing to the restriction of $F(t)^T F(t) \leq I$, the following inequalities can be obtained:

$$\begin{aligned} p^T(t, x(t), x(t-h(t)) p(t, x(t), x(t-h(t)))) &= \left[D_1 x(t) + D_2 x(t-h(t))\right]^T F^T(t) F(t) \left[D_1 x(t) + D_2 x(t-h(t))\right] \\ &\leq \left[D_1 x(t) + D_2 x(t-h(t))\right]^T \left[D_1 x(t) + D_2 x(t-h(t))\right]. \end{aligned} \tag{7}$$

Similarly, the load disturbance is considered as time-varying nonlinear function with current and delayed state vector as $C\Delta L_d(t) = g(t, x(t), x(t - h(t)))$, which satisfy the following norm-bounded constraints:

$$\|g(t, x(t), x(t-h(t)))\| \leq \rho \|x(t)\| + \tau \|x(t-h(t))\|, \tag{8}$$

$$\begin{aligned} &g^T(t, x(t), x(t-h(t))) g(t, x(t), x((t-h(t))) \\ &\quad \leq \rho^2 x^T(t) G^T G x(t) + \tau^2 x^T(t-h(t)) H^T H x(t-h(t)). \end{aligned} \tag{9}$$

where $\rho \geq 0$ and $\tau \geq 0$ represent known scalars. G and H represent known constant matrices with appropriate dimensions. ρ, τ, G, and H bound the magnitude of time-varying load disturbance of power system together.

3. Main Results

Before deriving the main results, Lemma 1 should be introduced. Lemma 1 bounds the integral of quadratic function multiplied by a 1st/2nd degree scalar function [26].

Lemma 1. *For a positive definite matrix M with appropriate dimensions and a vector $f(s)$, the following inequalities can be obtained for all scalar valued function $\kappa(s) \geq 0, s \in [t_1, t_2]$:*

$$-\int_{t_1}^{t_2} \kappa(s) f^T(s) M f(s) \mathrm{d}s \leq \alpha_1 \varepsilon_t^T F_1^T M^{-1} F_1 \varepsilon_t + 2\varepsilon_t^T F_1^T \int_{t_1}^{t_2} \kappa(s) f(s) \mathrm{d}s,$$
$$-\int_{t_1}^{t_2} \kappa^2(s) f^T(s) M f(s) \mathrm{d}s \leq \alpha_2 \varepsilon_t^T F_2^T M^{-1} F_2 \varepsilon_t + 2\varepsilon_t^T F_2^T \int_{t_1}^{t_2} \kappa(s) f(s) \mathrm{d}s. \tag{10}$$

where $\alpha_1 = \int_{t_1}^{t_2} \kappa(s)$ and $\alpha_2 = t_2 - t_1$. And F_1 and F_2 represent appropriate dimensional matrices and ε_t represents arbitrary vector. Then, we can obtain the delay-dependent robust stability criterion of system (3).

Theorem 1. *Given constants h and μ, the considered system (3) is asymptotically stable if there exist positive matrices $P_1, P_2 \in \mathbb{R}^{4n\times 4n}$, $Q_1, Q_2, Q_3 \in \mathbb{R}_+^{2n\times 2n}$, $L_1, L_2 \in \mathbb{R}_+^{n\times n}$, and any matrices $K_1, K_4 \in \mathbb{R}^{2n\times 9n}$ and $K_2, K_3, K_5, K_6 \in \mathbb{R}^{n\times 9n}$ satisfying the following LMIs:*

$$P_1 + h(t)P_2 > 0$$

$$\begin{bmatrix} \Omega_{\beta_1} & hK_1^T & hK_2^T & hK_3^T \\ \star & -hQ_3 & 0 & 0 \\ \star & \star & -L_1 & 0 \\ \star & \star & \star & -\frac{h}{3}L_2 \end{bmatrix} < 0,$$

$$\begin{bmatrix} \Omega_{\beta_2} & hK_1^T & hK_2^T & hK_3^T \\ \star & -hQ_3 & 0 & 0 \\ \star & \star & -L_1 & 0 \\ \star & \star & \star & -\frac{h}{3}L_2 \end{bmatrix} < 0,$$

$$\begin{bmatrix} \Omega_{\beta_3} & hK_3^T & hK_4^T & hK_5^T \\ \star & -hQ_3 & 0 & 0 \\ \star & \star & -L_1 & 0 \\ \star & \star & \star & -\frac{h}{3}L_2 \end{bmatrix} < 0, \tag{11}$$

$$\begin{bmatrix} \Omega_{\beta_4} & hK_3^T & hK_4^T & hK_5^T \\ \star & -hQ_3 & 0 & 0 \\ \star & \star & -L_1 & 0 \\ \star & \star & \star & -\frac{h}{3}L_2 \end{bmatrix} < 0,$$

where $\beta_1, \beta_2, \beta_3$, and β_4 represent $h(t) = 0$ and $\dot{h}(t) = -\mu$, $h(t) = 0$ and $\dot{h}(t) = \mu$, $h(t) = h$ and $\dot{h}(t) = -\mu$, and $h(t) = h$ and $\dot{h}(t) = \mu$, the four situations, respectively. Moreover, the details about other notations are listed in Appendix.

Proof. The Lyapunov functionals are adopted as follows:

$$\begin{aligned} V(t) = {} & \int_{t-h(t)}^{t} \left[\Xi_1^T(t,s) Q_1 \Xi_1(t,s) + \Xi_2^T(s) Q_1 \Xi_2(s)\right] \mathrm{d}s + \int_{t-h}^{t-h(t)} \left[\Xi_1^T(t,s) Q_2 \Xi_1(t,s) + \Xi_2^T(s) Q_2 \Xi_2(s)\right] \mathrm{d}s \\ & + \xi^T(t)\left(P_1 + h(t)P_2\right)\xi(t) + \int_{t-h}^{t} \left[(h - t + s)\Xi_2^T(s) Q_3 \Xi_2(s) + \dot{x}^T(s)\left((h - t + s)^2 L_1 + (h - t + s)^3 L_2\right)\dot{x}(s)\right] \mathrm{d}s, \end{aligned} \tag{12}$$

where $\xi(t) = [x^T(t), x^T(t - h(t)), x^T(t - h), \int_{t-h}^{t} x^T(s)\mathrm{d}s]^T$, $\Xi_1(t,s) = [x^T(t), x^T(s)]^T$, $\Xi_2(s) = [x^T(s), \dot{x}^T(s)]^T$.

Then, define $\zeta(t) \in \mathbb{R}^{9n\times 1}$ as $\zeta(t) = [x^T(t) x^T(t - h(t)) x^T(t - h) \int_{t-h}^{t-h(t)} x^T(s)\mathrm{d}s \int_{t-h(t)}^{t} x^T(s)\mathrm{d}s \quad \dot{x}^T(t - h(t)) \dot{x}^T(t - h), \ g^T(t, x(t), x((t - h(t)))) p^T \ (t, x(t), x \ (t - h(t)))]^T$; $\zeta^T(t) e_k^T$ represents the k th vector of $\zeta(t)$, e.g., $\zeta^T(t) e_1^T = x^T(t)$.

Computing the derivative of $V(t)$ along the trajectories of system (3):

$$\begin{aligned} \dot{V}(t) = {} & 2\xi^T(t)\left(P_1 + h(t)P_2\right)\dot{\xi}(t) + 2\int_{t-h(t)}^{t} \Xi_1^T(t,s) Q_1 \dot{\Xi}_1^T(t,s)\mathrm{d}s + 2\int_{t-h}^{t-h(t)} \Xi_1^T(t,s) Q_2 \dot{\Xi}_1(t,s)\mathrm{d}s + \dot{h}(t)\xi^T(t) P_2 \xi(t) \\ & + \Xi_1^T(t,t) Q_1 \Xi_1(t,t) + (1 - \dot{h}(t))\Xi_1^T(t, t - h(t))[Q_2 - Q_1]\Xi_1(t, t - h(t)) + \Xi_2^T(t)[Q_1 + hQ_3]\Xi_2(t) + h^2 \dot{x}^T(t) L_1 \dot{x}(t) \\ & + (1 - \dot{h}(t))\Xi_2^T(t - h(t))[Q_2 - Q_1]\Xi_2(t - h(t)) - \Xi_1^T(t, t - h) Q_2 \Xi_1(t, t - h) - \Xi_2^T(t - h) Q_2 \Xi_2(t - h) + h^3 \dot{x}^T(t) L_3 \dot{x}(t) \end{aligned}$$

$$\begin{aligned} &-\int_{t-h}^{t}\Xi_2^T(s)Q_3\Xi_2(s)\mathrm{d}s-2\int_{t-h}^{t}(h-t+s)\dot{x}^T(s)L_1\dot{x}(s)\mathrm{d}s-3\int_{t-h}^{t}(h-t+s)^2\dot{x}^T(s)L_2\dot{x}(s)\mathrm{d}s\\ &=\zeta^T(t)\Big(He\Big(G_1^T[P_1+h(t)P_2]G_2+G_3^TQ_1G_4+G_5^TQ_2G_6\Big)+\Pi\Big)\zeta(t)+f_a(t). \end{aligned} \tag{13}$$

The sum of all integral terms is expressed by $f_a(t)$:

$$f_a(t)=-\int_{t-h}^{t}\left\{\Xi_2^T(s)Q_3\Xi_2(s)+2(h-t+s)\dot{x}^T(s)L_1\dot{x}(s)+3(h-t+s)^2\dot{x}^T(s)L_2\dot{x}(s)\right\}\mathrm{d}s. \tag{14}$$

Owing to $-(h-t+s)\le-(h(t)-t+s),\forall s\in[t-h(t),t]$, the following inequalities can be obtained:

$$\begin{aligned} f_a(t)\le&-\int_{t-h}^{t-h(t)}\left\{\Xi_2^T(s)Q_3\Xi_2(s)+2(h(t)-t+s)\dot{x}^T(s)L_1\dot{x}(s)+3(h(t)-t+s)^2\dot{x}^T(s)L_2\dot{x}(s)\right\}\mathrm{d}s\\ &-\int_{t-h(t)}^{t}\left\{\Xi_2^T(s)Q_3\Xi_2(s)+2(h(t)-t+s)\dot{x}^T(s)L_1\dot{x}(s)+3(h(t)-t+s)^2\dot{x}^T(s)L_2\dot{x}(s)\right\}\mathrm{d}s\\ =&\Upsilon(t). \end{aligned} \tag{15}$$

Using Lemma 1 to estimate $\Upsilon(t)$:

$$\Upsilon(t)\le\zeta^T(t)\left\{\begin{array}{c}(h-h(t))K_1^TQ_3^{-1}K_1+2K_1^T(e_4,e_2-e_3)^T+(h-h(t))^2K_2^TL_1^{-1}K_2+4K_2^T[(h-h(t))e_2-e_4]^T\\ +3(h-h(t))K_3^TL_2^{-1}K_3+6K_3^T[(h-h(t))e_2-e_4]^T+h(t)K_4^TQ_3^{-1}K_4+2K_4^T[e_5,e_1-e_2]^T\\ +h^2(t)K_5^TL_1^{-1}K_5+4K_5^T[h(t)e_1-e_5]^T+3h(t)K_6^TL_2^{-1}K_6+6K_6^T(h(t)e_1-e_5)^T\end{array}\right\}\zeta(t). \tag{16}$$

The following inequality holds for any $\varsigma\ge0$ from (9) and (7), respectively:

$$\begin{aligned} -\varsigma g(.)^Tg(.)+\varsigma\rho^2x^T(t)G^TGx(t)+\varsigma\tau^2x^T(t-h(t))H^THx(t-h(t))\ge0,\\ -p(.)^Tp+[D_1x(t)+D_2x(t-h(t))]^T[D_1x(t)+D_2x(t-h(t))]\ge0. \end{aligned} \tag{17}$$

They can be expressed by the augmented state vector $\zeta(t)$, respectively:

$$\begin{aligned} \zeta^T(t)\Big(e_8^T(-\varsigma I)e_8+e_1^T\Big(\varsigma\rho^2G^TG\Big)e_1+e_2^T\Big(\varsigma\tau^2H^TH\Big)e_2\Big)\zeta(t)\ge0,\\ \zeta^T(t)e_9^T(-I)e_9+e_1^T\Big(D_1^TD_1\Big)e_1+e_1^T\Big(D_1^TD_2\Big)e_2+e_2^T\Big(D_2^TD_1\Big)e_1+e_2^T\Big(D_2^TD_2\Big)e_2\Big)\zeta(t)\ge0. \end{aligned} \tag{18}$$

By substituting (16) into (13) and adding the inequality (18), the following inequality can be obtained:

$$\dot{V}(t) \le \zeta^T(t)\left\{He\left(G_1^T P G_2 + G_3^T Q_1 G_4 + G_5^T Q_2 G_6 + H_1 + H_2 + H_3\right) + \Pi + \Lambda + \Psi\right\}\zeta(t), \tag{19}$$

where $G_1, G_2, G_3, G_4, G_5, G_6, H_1, H_2, H_3, \Lambda, \Pi$ have been defined in Appendix, and

$$\begin{aligned}\Psi = {} & (h - h(t))K_1^T Q_3^{-1} K_1 + (h - h(t))^2 K_2^T L_1^{-1} K_2 + 3(h - h(t))K_3^T L_2^{-1} K_3 \\ & + h(t)K_4^T Q_3^{-1} K_4 + h(t)H_5^T L_1^{-1} K_5 + 3h(t)K_6^T L_2^{-1} K_6.\end{aligned} \tag{20}$$

Finally, considering $0 \le h(t) \le h$ and $-\mu < \dot{h}(t) < \mu$, inequality (9) is obtained by Schur complement, which ensures the following inequality:

$$\begin{aligned}\dot{V}(t) &\le \zeta^T(t)\left\{He\left(G_1^T P G_2 + G_3^T Q_1 G_4 + G_5^T Q_2 G_6 + H_1 + H_2 + H_3\right) + \Pi + \Lambda + \Psi\right\}\zeta(t), \\ &< -\epsilon\|\zeta(t)\|^2. \exists \epsilon > 0, \\ &\le -\hat{\epsilon}\|x(t)\|^2. \exists \hat{\epsilon} > 0.\end{aligned} \tag{21}$$

Hence, the system is asymptotically stable. The proof is finished. □

Remark 2. The condition of positive matrices $P_1, P_2 \in \mathbb{R}^{4n\times 4n}$, $Q_1, Q_2, Q_3 \in \mathbb{R}_+^{2n\times 2n}$, and $L_1, L_2 \in \mathbb{R}_+^{n\times n}$ in Theorem 1 can guarantee the adopted Lyapunov functionals $V(t)$ being positive. Thus, the positive definite of $V(t)$ and negative definite of $\dot{V}(t)$ in time domain $[-h, 0]$ can guarantee the asymptotic stability of system (3) in $[-h, 0]$.

Remark 3. Our work has investigated the stability condition of LFC system (3) under the limitation $0 \le h(t) \le h$ and $-\mu \le \dot{h}(t) \le \mu$. The limitation conditions are $0 < h(t) < h, -\mu < \dot{h}(t) < \mu$. That is to say, the stability condition should be satisfied under the four situations, β_1: $h(t) = h_1, \dot{h}(t) = -\mu$, β_2: $h(t) = h_1, \dot{h}(t) = \mu$, β_3: $h(t) = h_2$, $\dot{h}(t) = -\mu$, and β_4: $h(t) = h_2, \dot{h}(t) = \mu$. $\dot{V}(t) < 0$ must be guaranteed under the four situations. Thus, inequality (9) under $\beta_1 - \beta_4$ in Theorem 1 must be satisfied simultaneously for system asymptotic stability.

Remark 4. The main contribution of this section is to propose a novel Theorem 1 in the form of LMIs which can derive a less conservative result of maximum allowable network delay for LFC system (3). The LKF constructed by literature [36] is $V(t) = x^T(t)Px(t) + \int_{t-\tau(t)}^{t} x^T(s)Q_1 x(s)\mathrm{d}s + \int_{t-\tau}^{t} x^T(s)Q_2 x(s)\mathrm{d}s + \tau\int_{-\tau}^{0}\int_{t+\theta}^{t}\dot{x}^T(s)R\dot{x}(s)\mathrm{d}s\mathrm{d}\theta$. Compared with that, the LKF proposed by this paper has four improvement points. (i) The augmented variable $[x^T(t), x^T(t-h(t)), x^T(t-h), \int_{t-h}^{t} x^T(s)\mathrm{d}s]^T$, rather than $x(t)$ in [36], which can reduce the conservatism by increasing the link between variables. (ii) The time-delay dependent matrix $P_1 + h(t)P_2$ is introduced in quadratic term, rather than constant matrix P in [36], which can reduce the conservatism by introducing more messages about time-varying delay. (iii) The cross terms of variable $\{x(t), x(s)\}, \{x(s), \dot{x}(s)\}$ in $\Xi_1(t,s), \Xi_2(t,s)$ also can reduce the conservatism by increasing the link between variables. (iv) The 4th, 5th, and 6th terms of the novel LKF multiplied by 1st, 2nd, and 3rd degrees of a scalar function $(h - t + s)$. The increasing of $(h - t + s)$ by one signifies the increasing the number of integral by one. Compared with the LKF of literatures [22, 36, 37], we increase the quadratic terms multiplied by 2nd and 3rd degrees of the scalar function $(h - t + s)$, which may reduce the conservatism compared with literatures [22, 36, 37].

Remark 5. If there is a small disturbance or no disturbed load in the LFC system, the delay-dependent robust stability criterion can be developed from Theorem 1 by setting $\rho = 0, \tau = 0$. If there is no or very small disturbance in LFC system parameters, set $N = 0$.

4. Case Studies

In this section, the typical single-area and two-area LFC systems are carried out to analyze the delay margins based on Theorem 1. The parameters of the real two-area LFC system are listed as Table 2. For verifying the less conservatism of our proposed method, the parameters of the two-area LFC system given in [37] are presented in Table 2 for comparison purposes. M, D, γ, T_g, T_t, and $\widehat{\nu}$ represent the

Table 2: Parameters of two-area LFC systems.

Parameter	T_t/s	T_g/s	$\widehat{v}$	D	γ	M/s	T_{12}
Area 1	0.3	0.1	0.05	1.0	21	10	0.1986
Area 2	0.4	0.17	0.05	1.5	21.5	12	

inertia moments of generator, the generator damping coefficient, the frequency bias factor, time constant of the governor, the turbine time constant, and the speed drop separately. Delay margins with respect to different value of ρ, τ, gains of PI controller are calculated for constant and time-varying time delays. Then, simulation studies based on MATLAB/Simulink are shown to investigate the effect of time delay on control performance and verify the improvement and effectiveness of the Theorem 1 proposed by this paper.

4.1. Theoretical Delay Margins

4.1.1. Single-Area LFC System. The parameters of Area 1 in Table 2 are adopted as single-area LFC system parameters.

Setting K_P as very small, we investigate the effect of Integral (I) controller on delay margin under three situations of load disturbance ($\rho = 0, \tau = 0$; $\rho = 0, \tau = 0.025$; and $\rho = 0.025, \tau = 0.025$) for both constant and time-varying delays. Suppose G and H in (9) and D_1 and D_2 in (8) as $0.1I_n$, where n represents the dimension of the system state vector $x(t)$. It can be seen that $n = 4$ in the single-area LFC system from (5). Theorem 1 is adopted to calculate the delay margins. The results are shown in Table 3 and Figures 2–4.

The following conclusions can be obtained from Table 3 and Figures 2–4:

(i) The increasing of ρ and τ represents that the load fluctuation becomes more pronounced. With the increase in ρ and τ, the delay margin that PI controller can withstand without decrease in losing stability under the same value of μ and K_I. The effect of load disturbance on delay-dependent stability of the LFC system can be obtained.

(ii) It can be seen from Figures 2–4 that the increasing of μ causes the decreasing of delay margin h with the same value of K_I under the three situations of load disturbance ($\rho = 0, \tau = 0$; $\rho = 0, \tau = 0.025$; $\rho = 0.025, \tau = 0.025$). The effect of time delay changing rate on delay-dependent stability of the LFC system can be obtained.

(iii) Simultaneously, it can be seen from Figures 2–4 that maximum allowable network delay decreases with the increasing of K_I with the same value of μ under the three situations of load fluctuation.

As for the nominal system condition ($\rho = 0, \tau = 0$) with constant ($\mu = 0$) and time-varying delay ($\mu = 0.9$), the maximum allowable network delays are listed in Table 4 compared with the other results from literatures [22, 36, 37]. It can be seen that the results calculated by Theorem 1 are less conservative than those of [22, 36, 37], owing to the progressiveness of Lyapunov functional and Lemma 1 adopted by this paper. Therefore, when compared with [22, 36, 37], the results proposed by this paper are more realistic.

Results of the maximum allowable network delays with regard to gains of PI controller (K_P, K_I) are listed in Table 5 and Figure 5 with constant delays ($\mu = 0$) and no load disturbance ($\rho = 0, \tau = 0$) and in Table 6 and Figure 6 with time-varying delays ($\mu = 0.9$) and load disturbance ($\rho = 0.025$, $\tau = 0.025$), separately. Results demonstrate that smaller h is obtained under the bigger K_P, K_I, and a relatively larger h is acquired for the smaller K_P, K_I. h is reduced with the increasing of K_P when $K_I \leq 0.05$. For $K_I \geq 0.1$, h increases at first and then decreases with the increasing of K_P. This results implies that for a given K_I, there is a optimal value of K_P which can acquire the maximum h, which can give guidance to tune PI controller to achieve maximum delay margins. Moreover, it can be found that h of the time-varying delays is smaller and decreases faster than that of constant delays.

4.1.2. Two-Area LFC System. Maximum allowable network delay (h) is calculated by Theorem 1 for the two-area LFC system listed in Table 2 by simplifying the multiple delay as a single delay like (3) and gains of PI controller for two areas as same ($K_{Pi} = K_P$, $K_{Ii} = K_I$). In the two-area LFC system, both the values of G, H, D_1, and D_2 are taken as $0.1I_n$, where $n = 9$.

In two-area LFC system case, for more clearly comparisons with literatures [22, 36, 37], the results are summarized in Table 7 with the condition of ($\rho = 0, \tau = 0$) under constant ($\mu = 0$) and time-varying delay ($\mu = 0.5$). Similarity, the listed results are less conservative than those of [22, 36, 37]. Also, the results of Table 7 show the effect of PI controller gains on the delay margins.

Also, the results of delay margin with respect to gains of PI controller are listed in Table 8 and Figure 7 with constant delay ($\mu = 0$) and no load fluctuation ($\rho = 0, \tau = 0$) and in Table 9 and Figure 8 with time-varying delay ($\mu = 0.9$) and load fluctuation ($\rho = 0.025, \tau = 0.025$), respectively. The delay margin changing trend with regard to gains of PI controller of the two-area LFC system is consistent with that of the single-area LFC system. Hence, the details can be omitted here.

4.2. Simulation Verification.

The models of the single-area and two-area LFC system are built in MATLAB/Simulink separately. The simulation results verify the above calculation results. The state vectors (Δf) are selected as the observation since the load fluctuation directly affects the frequency of the LFC system.

Table 3: Delay margin $h \propto K_I$ under three situations of load disturbance (single-area LFC).

K_I		0.05	0.1	0.2	0.4	0.6	1
$\rho = 0 \quad \tau = 0$	$\mu = 0$	32.89	15.752	7.82	3.8213	2.214	0.9824
	$\mu = 0.5$	25.178	10.818	5.812	2.813	1.5123	0.5812
$\rho = 0, \tau = 0.025$	$\mu = 0$	26.124	12.453	6.512	3.541	2.112	0.8721
	$\mu = 0.5$	24.981	9.718	4.774	2.572	1.417	0.4882
$\rho = 0.025, \tau = 0.025$	$\mu = 0$	25.516	12.011	5.918	3.211	1.812	0.743
	$\mu = 0.5$	23.828	7.521	3.514	2.012	1.228	0.334

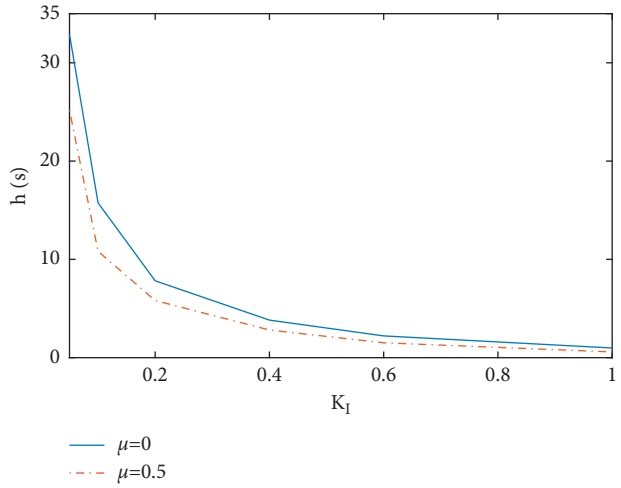

Figure 2: Delay margin $h \propto K_I$ for single-area with $(\rho = 0, \tau = 0)$.

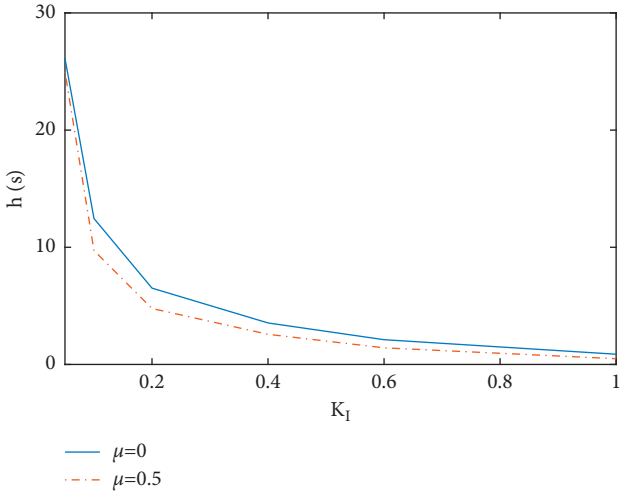

Figure 3: Delay margin $h \propto K_I$ for single-area with $(\rho = 0, \tau = 0.025)$.

4.2.1. Single-Area LFC System. It can be seen from Table 4 that the maximum allowable network delay calculated by Theorem 1 is $h = 6.64$ under the condition of $\rho = \tau = 0, \mu = 0.9, K_P = 0.1, K_I = 0.2$. The time-varying delay $h(t)$ is supposed to be a sine function $h(t) = 3.32 + 3.32\sin(0.27t)$. Figure 9 shows that the state vector Δf converges asymptotically to stable point for $h = 6.64$; however, the delay margin calculated by [22] is 4.67, calculated by [36] is 5.94, and calculated by [37] is 6.59. Moreover, if h exceeds beyond 6.64, the system becomes unstable as shown in Figure 10 for $h = 7s$.

4.2.2. Two-Area LFC System. At first, when $h(t) = 0$, the state-space model of two-area LFC system becomes $\dot{x}(t) = (A + \Delta A + B + \Delta B)x(t) + C\Delta L_d(t)$. Figure 11 shows that the delay-free system is asymptotically stable. It can be seen from Table 9 that the maximum allowable delay

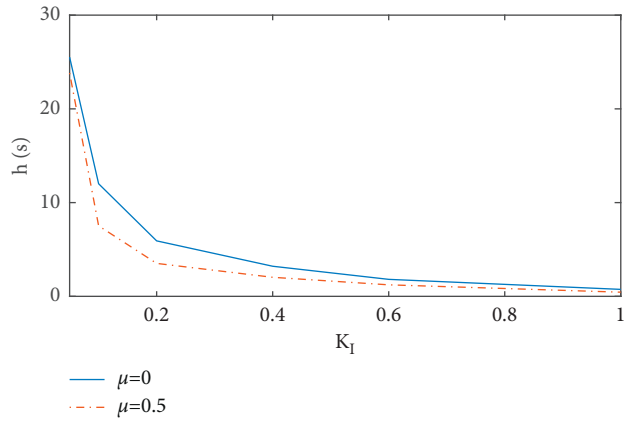

Figure 4: Delay margin $h \propto K_I$ for single-area with $(\rho = 0.025, \tau = 0.025)$.

Table 4: Delay margin h by Theorem 1 for single-area LFC with $\varrho = 0, \tau = 0$.

K_P		0	0	0	0	0	0.1	0.1	0.1	0.1	0.1
K_I		0.05	0.2	0.4	0.6	1	0.05	0.2	0.4	0.6	1
$\mu = 0$	Theorem 1	32.89	7.82	3.8213	2.214	0.9824	32.98	7.89	3.83	2.29	1.12
	[22]	27.92	6.69	3.12	1.91	0.88	27.03	6.94	3.29	2.02	0.96
	[36]	27.92	6.69	3.12	1.91	0.88	27.05	6.94	3.29	2.02	0.96
	[37]	30.91	7.33	3.38	2.04	0.92	31.61	7.79	3.61	2.19	1.01
$\mu = 0.9$	Theorem 1	27.87	6.54	3.02	1.82	0.78	22.84	6.64	3.14	1.86	0.79
	[22]	20.45	4.59	1.81	1.011	0.48	17.39	4.67	1.85	1.05	0.48
	[36]	26.37	6.25	2.85	1.68	0.74	20.25	5.94	2.87	1.75	0.74
	[37]	27.26	6.43	2.91	1.71	0.75	22	6.59	3.11	1.84	0.75

Table 5: Delay margin $h \propto (K_P, K_I)$ for single-area LFC with $\mu = 0, \rho = 0, \tau = 0$.

h	K_P						
K_I	0	0.05	0.1	0.2	0.4	0.6	1
0.05	32.89	31.72	30.98	28.312	26.424	25.124	20.818
0.1	16.43	14.34	16.89	15.24	10.24	5.71	2.14
0.15	9.23	8.82	9.51	8.92	4.14	1.56	0.75
0.2	7.82	6.23	7.89	7.899	3.12	1.52	0.54
0.4	3.8213	2.413	3.83	4.21	3.02	1.42	0.32
0.6	2.214	1.812	2.29	3.31	3.01	1.02	0.12
1	0.9824	0.813	1.12	2.32	2.48	0.83	0.08

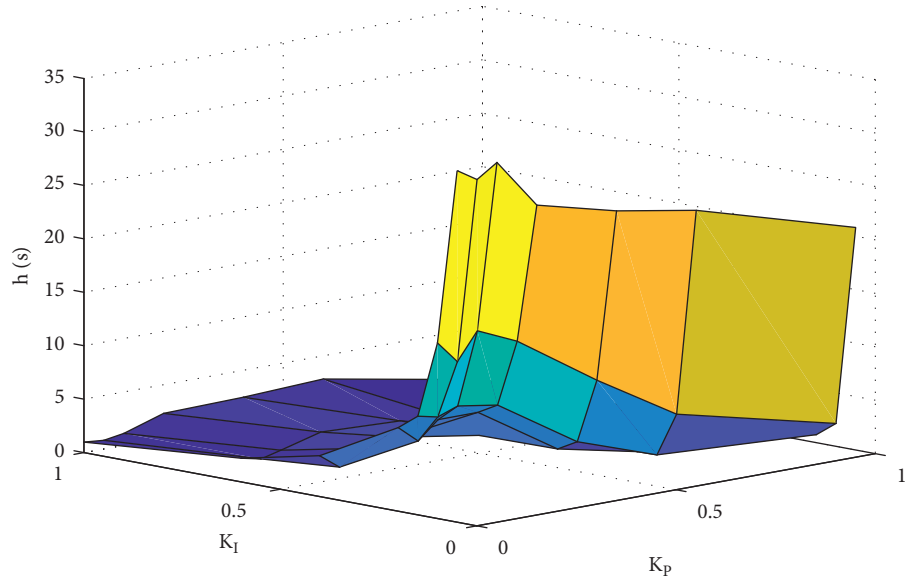

Figure 5: $h \propto (K_P, K_I)$ (single-area with $\mu = 0, \rho = 0, \tau = 0$).

Table 6: Delay margin $h \propto (K_P, K_I)$ for single-area LFC with $\mu = 0.9, \rho = 0.025, \tau = 0.025$.

h	K_P						
K_I	0	0.05	0.1	0.2	0.4	0.6	1
0.05	22.541	21.031	19.383	12.541	2.84	2.6	0.531
0.1	11.830	12.163	11.164	7.802	2.823	2.54	0.527
0.15	8.13	8.153	8.063	6.142	2.804	2.52	0.519
0.2	6.584	7.702	6.472	5.234	2.784	2.11	0.511
0.4	3.612	3.923	3.842	3.436	2.684	2.01	0.5
0.6	2.011	2.048	2.052	1.943	1.67	0.98	0.48
1.0	0.821	0.727	0.741	0.799	0.68	0.54	0.44

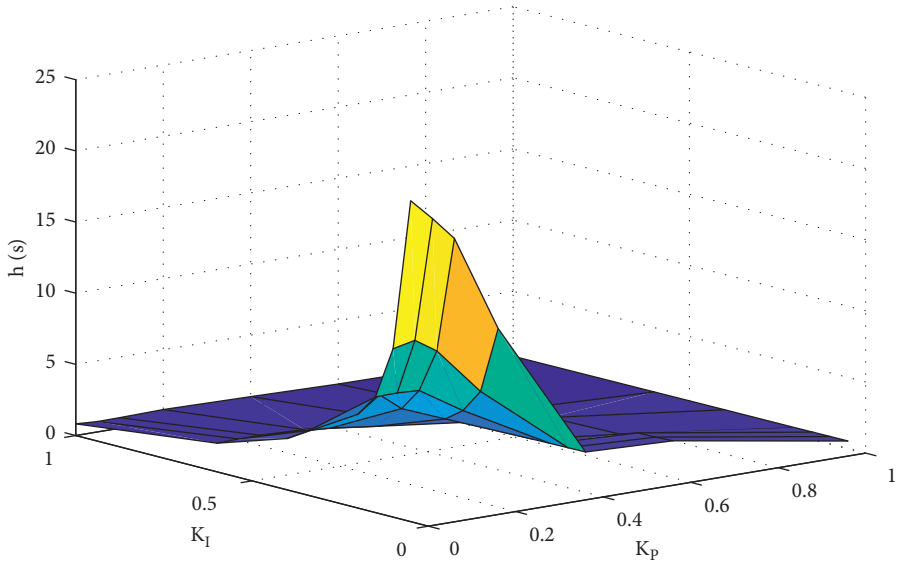

Figure 6: $h \propto (K_P, K_I)$ (single-area with $\mu = 0.9, \rho = 0.025, \tau = 0.025$).

Table 7: Delay margin h by Theorem 1 for two-area LFC with $\varrho = 0, \tau = 0$.

K_P		0	0	0	0	0.1	0.1	0.1
K_I		0.2	0.4	0.6	1	0.2	0.4	0.6
$\mu = 0$	Theorem 1	7.51	3.54	2.1	0.82	7.81	3.52	2.31
	[22]	6.6	3	1.74	0.57	6.88	3.17	1.86
	[36]	6.6	3	1.74	0.57	6.88	3.17	1.86
	[37]	7.23	3.24	1.86	0.58	7.67	3.47	2.01
$\mu = 0.5$	Theorem 1	6.52	2.92	1.84	0.52	6.81	2.92	1.82
	[22]	5.55	2.36	1.18	0.22	5.35	2.55	1.3
	[36]	6.14	2.68	1.4	0.35	6.34	2.83	1.51
	[37]	6.41	2.81	1.54	0.41	6.75	2.84	1.53

Table 8: Delay margin $h \propto (K_P, K_I)$ for two-area LFC with $\mu = 0, \varrho = 0, \tau = 0$.

h	K_P						
K_I	0	0.05	0.1	0.2	0.4	0.6	1
0.05	28.442	28.387	27.521	26.19	21.012	15.328	0.564
0.1	14.699	14.821	14.250	13.782	11.012	8.332	0.464
0.15	9.234	9.524	9.262	8.772	8.014	5.021	0.444
0.2	7.51	7.82	7.93	6.872	5.823	4.621	0.433
0.4	3.54	3.72	3.81	3.92	2.92	2.01	0.384
0.6	2.1	2.24	2.41	2.58	2.24	1.89	0.342
1	0.81	0.92	0.98	1.02	0.92	0.81	0.227

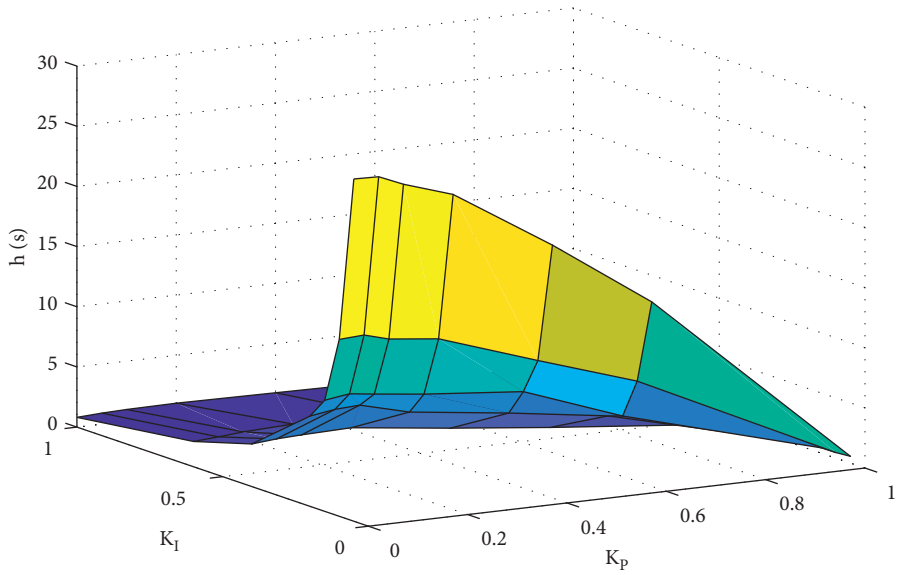

Figure 7: $h \propto (K_P, K_I)$ (two-area LFC with $\mu = 0, \rho = 0, \tau = 0$).

Table 9: Delay margin $h \propto (K_P, K_I)$ for two-area LFC with $\mu = 0.9, \varrho = 0.025, \tau = 0.025$.

h	K_P						
K_I	0	0.05	0.1	0.2	0.4	0.6	1
0.05	24.982	23.982	23.012	21.475	14.464	0.924	0.328
0.1	12.754	13.071	12.63	11.421	7.745	0.912	0.32
0.15	7.917	8.27	8.012	7.259	4.905	0.823	0.312
0.2	6.55	6.97	7.02	6.78	4.62	0.79	0.304
0.4	2.472	2.672	2.854	2.541	1.824	0.62	0.272
0.6	1.92	2.01	2.34	2.48	1.02	0.52	0.24
1	0.32	0.34	0.38	0.4	0.41	0.25	0.172

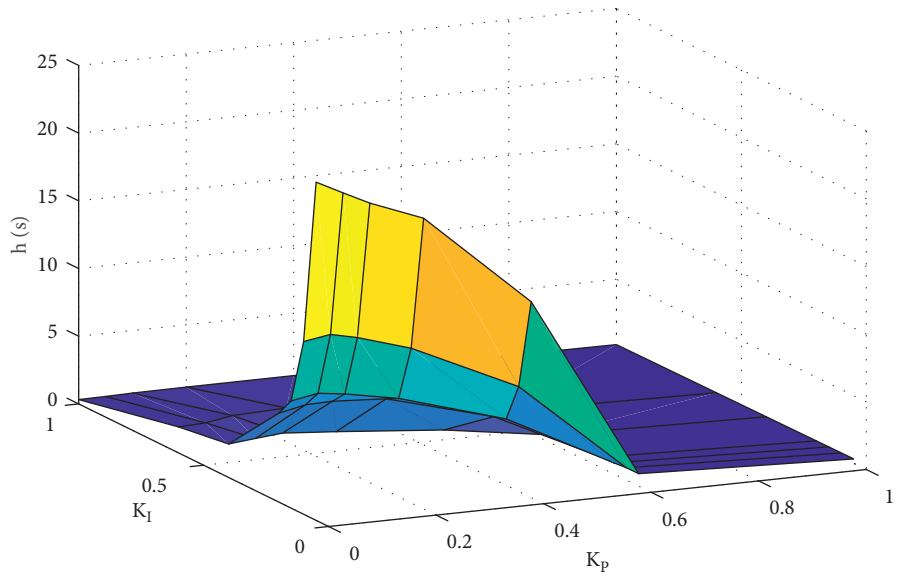

Figure 8: $h \propto (K_P, K_I)$ (two-area LFC with $\mu = 0.9, \rho = 0.025, \tau = 0.025$).

calculated by Theorem 1 is $h = 6.78$ under the condition of $\rho = \tau = 0.025, \mu = 0.9, K_P = K_I = 0.2$. Then, it can be seen from Figure 11 that the two-area LFC system is asymptotically stable under $h = 6.78$. Moreover, if h exceeds beyond 6.78, the system becomes unstable as shown in Figure 12 for $h = 7s$.

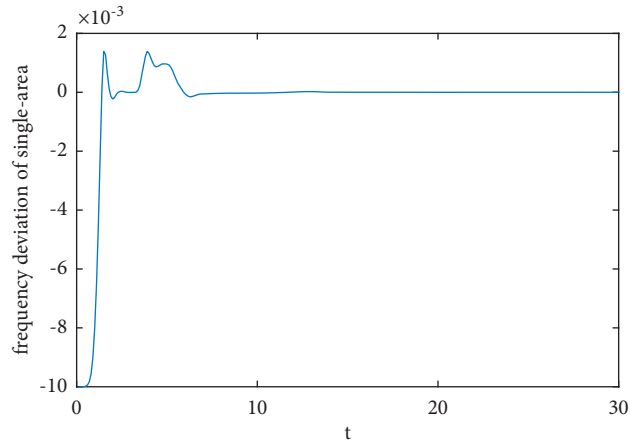

Figure 9: Frequency responses with $h = 6.64\,(\mu = 0.9)$ of single-area.

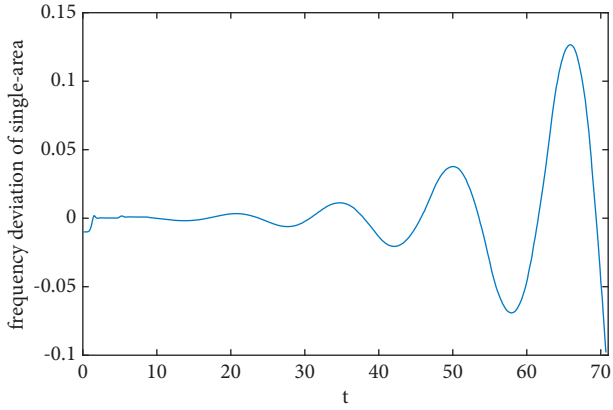

Figure 10: Frequency responses with $h = 7$ of single-area.

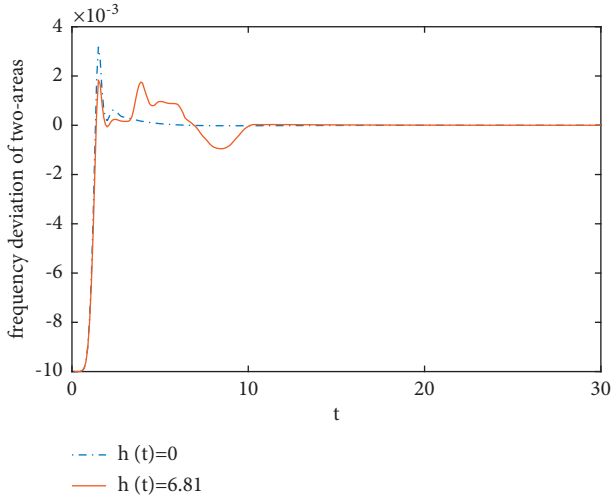

Figure 11: Frequency responses with $h = 6.81\,(\mu = 0.5)$ and without delay of two areas.

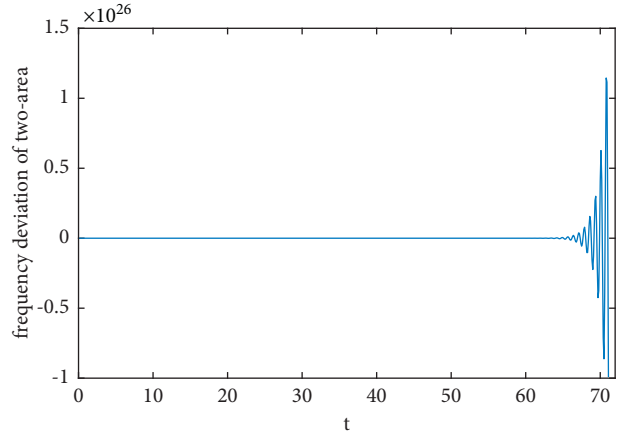

Figure 12: Frequency responses with $h = 7$ of two areas.

5. Conclusion

The stability criterion for the time-varying delay LFC system with nonlinearly load disturbance and random disturbance of system parameters has been investigated by adopting a novel simple LKF and integral inequality (Lemma 1). Considering the exogenous load disturbance and random disturbance of system parameters as constrained nonlinearly function, a time-varying delay system is modeled to describe the delayed LFC system. The novel simple LKF includes delay-dependent matrix in quadratic term, cross terms of variables, and quadratic terms multiplied by 1st, 2nd, and 3rd degrees of scalar function. Lemma 1 is adopted to bound the quadratic terms multiplied 1st and 2nd degrees of scalar function emerging in the derivative of LKF. The results of the novel simple LKF contributing to reduce conservatism and the relationships between the time delay varying rate, load disturbance degree, the gains of PI controller, and delay

margins are derived by the case studied. Meanwhile, simulation verifies the effectiveness and superiority of our results. Nevertheless, the security threats in actual communication network such as denial of service (DOS) attacks and deception attacks are not considered in our work. In the future, how to analyze the stability of the LFC system under the simultaneous existence of various network attack, such as DOS and deception attacks, will be the focus of our following work.

Appendix

$$
\begin{aligned}
\Omega &= He\left(G_1^T\left(P_1 + h(t)P_2\right)G_2 + G_3^T Q_1 G_4 + G_5^T Q_2 G_6 + H_1 + H_2 + H_3\right) + \Pi + \Lambda,\\
G_1 &= \left[e_1^T e_2^T e_3^T e_4^T + e_5^T\right]^T,\\
G_2 &= \left[A_c^T e_6^T e_7^T e_1^T - e_3^T\right]^T,\\
G_3 &= \left[h(t)e_1^T e_5^T\right]^T,\\
G_4 &= \left[A_c^T e_0^T\right]^T,\\
G_5 &= \left[(h - h(t))e_1^T e_4^T\right]^T,\\
G_6 &= \left[A_c^T e_0^T\right]^T,\\
H_1 &= \left[e_4^T e_2^T - e_3^T\right]K_1 + \left[e_5^T e_1^T - e_2^T\right]K_4,\\
H_2 &= 2\left((h - h(t))e_2^T - e_4^T\right)K_2 + 2\left(h(t)e_1^T - e_5^T\right)K_5,\\
H_3 &= 3\left((h - h(t))e_2^T - e_4^T\right)K_3 + 3\left(h(t)e_1^T - e_5^T\right)K_6,\\
\Pi &= \dot{h}(t)\left[e_1^T e_2^T e_3^T e_4^T + e_5^T\right]P_2\left[e_1^T e_2^T e_3^T e_4^T + e_5^T\right]^T + \left[e_1^T e_1^T\right]Q_1\left[e_1^T e_1^T\right]^T - (1 - \dot{h}(t))\left[e_1^T e_2^T\right]Q_1\left[e_1^T e_2^T\right]^T\\
&\quad + \left[e_1^T A_c^T\right]Q_1\left[e_1^T A_c^T\right]^T - (1 - \dot{h}(t))\left[e_2^T e_6^T\right]Q_1\left[e_2^T e_6^T\right]^T + (1 - \dot{h}(t))\left[e_1^T e_2^T\right]Q_2\left[e_1^T e_2^T\right]^T - \left[e_1^T e_3^T\right]Q_2\left[e_1^T e_3^T\right]^T\\
&\quad + (1 - \dot{h}(t))\left[e_2^T e_6^T\right]Q_2\left[e_2^T e_6^T\right]^T - \left[e_3^T e_7^T\right]Q_2\left[e_3^T e_7^T\right]^T + h\left[e_1^T A_c^T\right]Q_3\left[e_1^T A_c^T\right]^T + A_c^T\left(h^2 L_1 + h^3 L_2\right)A_c,\\
\Lambda &= -e_8^T(\varsigma I)e_8 + e_1^T\left(\varsigma\rho^2 G^T G\right)e_1 + e_2^T\left(\varsigma\tau^2 H^T H\right)e_2 - e_9^T(I)e_9 + e_1^T\left(D_1^T D_1\right)e_1 + e_1^T\left(D_1^T D_2\right)e_2 + e_2^T\left(D_2^T D_1\right)e_1 + e_2^T\left(D_2^T D_2\right)e_2,\\
e_i &= \left[0_{n\times(i-1)n}\, I_n\, 0_{n\times(9-i)n}\right] \quad i = 1, 2, \ldots, 9,\\
e_0 &= 0_{n\times 9n},\\
A_C &= [\mathrm{AB}0_{n\times 5n} I_n N].
\end{aligned}
\tag{A.1}
$$

Data Availability

The raw/processed data required to reproduce these findings cannot be shared at this time as the data also form part of an ongoing study.

Conflicts of Interest

The authors declare that there are no conflicts of interest.

Authors' Contributions

The manuscript was approved by all authors for publication.

Acknowledgments

This work was supported by the National Natural Science Foundation of China under Grant Nos. 61703060, 12061088, 61802036, and 61873305, the Sichuan Science and Technology Program under Grant No. 21YYJC0469, the project funded by China Postdoctoral Science Foundation under Grant Nos. 2020M683274 and 2021T140092, the Open Research Project of the State Key Laboratory of Industrial Control Technology, Zhejiang University, China, under Grant No. ICT2021B38, the Guangdong Basic and Applied Basic Research Foundation under Grant No. 2021A1515011692, and the Central Government Funds of Guiding Local Scientific and Technological Development for Sichuan Province of China under Grant No. 2021ZYD0012.

References

[1] A. Naveed, Ş. Sönmez, and S. Ayasun, "Impact of electric vehicle aggregator with communication time delay on stability regions and stability delay margins in load frequency

control system," *Journal of Modern Power Systems and Clean Energy*, vol. 9, no. 3, pp. 595–601, 2021.

[2] H. Bevrani, A. Ghosh, and G. Ledwich, "Renewable energy sources and frequency regulation: survey and new perspectives," *IET Renewable Power Generation*, vol. 4, no. 5, pp. 438–457, 2010.

[3] I. P. Kumar and D. P. Kothari, "Recent philosophies of automatic generation control strategies in power system," *IEEE Transactions on Power Systems*, vol. 20, pp. 346–357, 2005.

[4] P. S. Kundur, *Power System Stability and Control*, McGraw-Hill, New York, USA, 1994.

[5] H. Bevrani, *Robust Power System Frequency Control*, Springer, New York, USA, 2009.

[6] F. W, K. Moslehi, and A. Bose, "Power system control centers: past, present, and future," *Proceedings of the IEEE*, vol. 93, no. 11, pp. 1890–1908, 2005.

[7] K. Shi, Y. Tang, X. Liu, and S. Zhong, "Secondary delay-partition approach on robust performance analysis for uncertain time-varying Lurie nonlinear control system," *Optimal Control Applications and Methods*, vol. 38, no. 6, pp. 1208–1226, 2017.

[8] K. Shi, Y. Tang, X. Liu, and S. Zhong, "Non-fragile sampled-data robust synchronization of uncertain delayed chaotic Lurie systems with randomly occurring controller gain fluctuation," *ISA Transactions*, vol. 66, pp. 185–199, 2017.

[9] K. Shi, Y. Tang, S. Zhong, C. Yin, X. G. Huang, and W. Wang, "Nonfragile asynchronous control for uncertain chaotic Lurie network systems with Bernoulli stochastic process," *International Journal of Robust and Nonlinear Control*, vol. 28, no. 5, pp. 1693–1714, 2018.

[10] K. Shi, J. Wang, Y. Tang, and S. Zhong, "Reliable asynchronous sampled-data filtering of T-S fuzzy uncertain delayed neural networks with stochastic switched topologies," *Fuzzy Sets and Systems*, vol. 381, no. 15, pp. 1–25, 2020.

[11] K. Shi, J. wang, S. Zhong, Y. Tang, and J. Cheng, "Non-fragile memory filtering of T-S fuzzy delayed neural networks based on switched fuzzy sampled-data control," *Fuzzy Sets and Systems*, vol. 394, pp. 40–64, 2020.

[12] F. Milano and M. Anghel, "Impact of time delays on power system stability," *IEEE Transactions on Circuits and Systems I: Regular Papers*, vol. 59, no. 4, pp. 889–900, 2012.

[13] S. Wang, X. Meng, and T. Chen, "Wide-area control of power systems through delayed network communication," *IEEE Transactions on Control Systems Technology*, vol. 20, no. 2, pp. 495–503, 2012.

[14] A. Sargolzaei, K. K. Yen, and M. N. Abdelghani, "Preventing time-delay switch attack on load frequency control in distributed power systems," *IEEE Transactions on Smart Grid*, vol. 7, pp. 1–10, 2015.

[15] S. Wen, X. Yu. Z. Zeng, and J. Wang, "Event-triggering load frequency control for multi area power systems with communication delays," *IEEE Transactions on Industrial Electronics*, vol. 63, no. 2, pp. 1308–1317, 2016.

[16] V. P. Singh and N Kishor, "Load frequency control with communication topology changes in smart grid," *IEEE Transactions on Industrial Informatics*, vol. 12, no. 5, pp. 1943–1952, 2016.

[17] S. Sonmez, S. Ayasun, and C. O. Nwankpa, "An exact method for computing delay margin for stability of load frequency control systems with constant communication delays," *IEEE Transactions on Power Systems*, vol. 31, no. 1, pp. 370–377, 2016.

[18] H. J. Jia and X. D. Yu, "A simple method for power system stability analysis with multiple time delays," in *Proceedings of the 2008 IEEE Power and Energy Society General Meeting - Conversion and Delivery of Electrical Energy in the 21st Century*, pp. 20–24, Pittsburgh, PA, USA, July 2008.

[19] N. Olgac and R. Sipahi, "An exact method for the stability analysis of time-delayed linear time-invariant (LTI) systems," *IEEE Transactions on Automatic Control*, vol. 47, no. 5, pp. 793–797, 2002.

[20] R. Sipahi and N. Olgac, "Complete stability robustness of third-order LTI multiple time-delay systems," *Automatica*, vol. 41, no. 8, pp. 1413–1422, 2005.

[21] Z. Y. Liu, C. Z. Zhu, and Q. Y. Jiang, "Stability analysis of time delayed power system based on cluster treatment of characteristic roots method," in *Proceedings of the 2008 IEEE Power and Energy Society General Meeting - Conversion and Delivery of Electrical Energy in the 21st Century*, pp. 20–24, Pittsburgh, PA, USA, July 2008.

[22] L. Jiang, W. Yao, Wu, Wen, and Cheng, "Delay-dependent stability for load frequency control with constant and time-varying delays," *IEEE Transactions on Power Systems*, vol. 27, no. 2, pp. 932–941, 2012.

[23] C. K. Zhang, L. Jiang, Wu, Y. He, and M. Wu, "Further results on delay-dependent stability of multi-area load frequency control," *IEEE Transactions on Power Systems*, vol. 28, no. 4, pp. 4465–4474, 2013.

[24] F. Yang, J. He, and Q. Pan, "Further improvement on delay-dependent load frequency control of power systems via truncated B-L inequality," *IEEE Transactions on Power Systems*, vol. 33, no. 5, pp. 5062–5071, 2018.

[25] K. S. Ko and D. K. Sung, "The effect of EV aggregators with time-varying delays on the stability of a load frequency control system," *IEEE Transactions on Power Systems*, vol. 33, no. 1, pp. 669–680, 2018.

[26] J. H. Kim, "Note on stability of linear systems with time-varying delay," *Automatica*, vol. 47, pp. 2118–2121, 2011.

[27] E. Fridman, U. Shaked, and K. Liu, "New conditions for delay-derivative-dependent stability," *Automatica*, vol. 45, no. 11, pp. 2723–2727, 2009.

[28] J. Sun, G. Liu, J. Chen, and D. Rees, "Improved delay-range-dependent stability criteria for linear systems with time-varying delays," *Automatica*, vol. 46, no. 2, pp. 466–470, 2010.

[29] Y. He, Q. G. Wang, L. H. Xie, and C. Lin, "Further improvement of free-weighting matrices technique for systems with time-varying delay," *IEEE Transactions on Automatic Control*, vol. 52, no. 2, pp. 293–299, 2007.

[30] A. Seuret and F. Gouaisbaut, "Wirtinger-based integral inequality: application to time-delay systems," *Automatica*, vol. 49, no. 9, pp. 2860–2866, 2013.

[31] P. G. Park, W. I. Lee, and S. Y. Lee, "Auxiliary function-based integral inequalities for quadratic functions and their applications to time-delay systems," *Journal of the Franklin Institute*, vol. 352, no. 4, pp. 1378–1396, 2015.

[32] F. Yang and H. Zhang, "T-S model-based relaxed reliable stabilization of networked control systems with time-varying delays under variable sampling," *International Journal of Fuzzy Systems*, vol. 13, pp. 260–269, 2011.

[33] C. K. Zhang, L. Jiang, Q. H. Wu, Y. He, and M. Wu, "Delay-dependent robust load frequency control for time-delay power systems," *IEEE Transactions on Power Systems*, vol. 28, no. 3, pp. 2192–2201, 2013.

[34] K. Ramakrishnan, "Improved results on delay-dependent stability of LFC systems with multiple time-delays," *Journal of Control, Automation and Electrical Systems*, vol. 26, no. 3, pp. 235–240, 2015.

[35] H. C. Luo, I. A. Hiskens, and Z. Hu, "Stability analysis of load frequency control systems with sampling and transmission delay," *IEEE Transactions on Power Systems*, vol. 35, no. 5, pp. 3603–3615, 2020.

[36] K. Ramakrishnan and G. Ray, "Stability criteria for nonlinearly perturbed load frequency systems with time-delay," *IEEE Journal on Emerging and Selected Topics in Circuits and Systems*, vol. 5, no. 3, pp. 383–392, 2015.

[37] F. S. Yang, J. He, and D. H. Wang, "New stability criteria of delayed load frequency control systems via infinite-series-based inequality," *IEEE Transactions on Industrial Informatics*, vol. 14, no. 1, pp. 231–240, 2018.